Electronic Supporting Information for:

Carbon-titanium dioxide (C/TiO_2) nanofiber composites for chemical oxidation of emerging organic contaminants in reactive filtration applications

Katherine E. Greenstein,[1] Matthew Nagorzanski,[1] Bailey Kelsay,[1] Edgard M. Verdugo,[1] Nosang V. Myung,[2] Gene F. Parkin,[1] David M. Cwiertny[1,3*]

[1]Department of Civil and Environmental Engineering, University of Iowa, Iowa City, IA 52242
[2]Department of Chemical and Biomolecular Engineering, University of Notre Dame, South Bend, IN, 46556
[3]Department of Chemical and Biochemical Engineering, University of Iowa, Iowa City, IA 52242

*Corresponding Author Contact Information:
David M. Cwiertny
Address: 4105 Seamans Center
University of Iowa, Iowa City, IA 52242
E-mail: david-cwiertny@uiowa.edu
Phone: 319-335-1401
Fax: 319-335-5660

Prepared for *Environmental Science: Nano*

January 31, 2021

15 Figures and 21 Pages

Electronic Supporting Information contains additional information related to synthesis, characterization, and reactivity experimental methods and additional results related to reactivity of nanofiber composites investigated herein.

SUPPLEMENTAL MATERIALS AND METHODS

Reagents. All chemicals were reagent grade or better and used as received. The synthesis of the C/TiO_2 nanofibers involved *N,N*-dimethylformamide (DMF) (BDH, 99.8%), polyacrylonitrile (PAN) (Aldrich, MW 150,000), Aeroxide® P25 (Acros Organics), 5 nm anatase TiO_2 nanoparticles (U.S. Research Nanomaterials, Inc., 99.5%), and phthalic acid (PTA) (Sigma Aldrich, 99.5+%). The buffer used in all photochemical experiments was 5 mM potassium phosphate monobasic (Fisher Scientific, 99.3%) with pH adjusted to 7. The target suite of organic micropollutants included atrazine (Fluka, 99.1%), 1H-benzotriazole (Alfa Aesar, 99%), caffeine (Sigma-Aldrich, 99+%), carbamazepine (Sigma-Aldrich, 98+%), *N,N*-diethyl-meta-toluamide (DEET) (Sigma-Aldrich, 97.6%), metoprolol tartrate (LKT Laboratories, 98+%), naproxen (Sigma-Aldrich, 99+%), and sulfamethoxazole (Sigma-Aldrich, 99+%). The synthesis of gold nanoparticles deposited on titanium dioxide nanoparticles involved gold (III) chloride trihydrate (Sigma-Aldrich, 99.9%) and L-ascorbic acid (Sigma-Aldrich, 99%). The eluents for HPLC analyses of micropollutants contained potassium phosphate monobasic (Fisher Scientific, 99.3%), acetonitrile (Fisher Scientific, 99.9%), and methanol (Fisher Scientific, 99.9%). All solutions were prepared in deionized (DI) water (Millipore, Milli-Q).

Synthesis of Au/TiO_2 particles. First, 0.3 g of P25 nanoparticles were suspended in 150 mL of 1 mM gold chloride solution. The ratio of gold salt concentration to P25 nanoparticles in suspension was prepared at the desired Au loading of 1.5 wt%, assuming complete deposition from solution. Next, 3 mL of 10 mM ascorbic acid was added drop wise to the suspension to reduce soluble Au^{3+} to metallic Au(0). The mixture was left to stir for one day, then the resulting particles were washed and dried.

Nanofiber filter characterization. Nanofiber diameter, TiO_2 distribution, and porosity were investigated with a Hitachi S-4800 scanning electron microscope (SEM).[1] To prepare for SEM, a 0.5 cm by 0.5 cm piece of a nanofiber mat was placed on carbon tape on Al sample stubs and subsequently sputter-coated with Au to reduce charging while imaging. To prepare samples for cross-sectional imaging using SEM, a 0.5 cm by 0.5 cm piece of nanofiber mat was sandwiched between pieces of cardboard with carbon tape for support, with the cardboard holding the samples subsequently carbon taped to Al stubs. The phase of TiO_2 nanoparticles was confirmed with X-ray diffraction (XRD, Rigaku MiniFlexII, Co X-ray source). For XRD, a 0.5 cm by 0.5 cm piece of nanofiber mat was taped to a glass slide with 0.2 mm well depth and analyzed from 20°C to 80°C for Bragg angle. N_2-BET analysis (Quantachrome Nova 4200e) was used to determine surface area of nanofiber composites after outgassing samples at 60°C for 6 h prior to measurement. Relative abundance of Ti on the surface of nanofibers was analyzed with a Kratos Axis Ultra X-ray photoelectron spectroscopy (XPS) system equipped with a monochromatic Al Kα X-ray source. For XPS analysis, approximately 0.5 cm by 0.5 cm of C/TiO_2 was placed on a sample holder using carbon tape. XPS was used to collect full spectrum survey scans, as well as to examine O 1s, C 1s, N 1s, and Ti 2p regions.

Preparation of organic micropollutant aqueous stock solutions. Saturated stock solutions of 110 μM (24 mg/L) atrazine, 125 μM (30 mg/L) carbamazepine, 80 μM (16 mg/L) naproxen, and 1 mM (253 mg/L) sulfamethoxazole were prepared in DI water by adding each constituent to a level above the solubility limit in water, stirring overnight, and using vacuum filtration with 0.22 μm nitrocellulose filters (Millipore) for removal of any residual, undissolved solids. Because of their higher solubility in water, stock solutions of benzotriazole, DEET,

caffeine, and metoprolol were prepared directly in DI water (at 10 mM, 1 mM, 5 mM, and 10 mM, respectively).

Analytical Methods. During filtration experiments, 0.5 mL samples were placed in 2 mL amber autosampler vials that were crimp sealed prior to analysis. All HPLC methods were adapted from previous work.[1,2] Briefly, atrazine samples were analyzed at 223 nm with an eluent of 50% acetonitrile/50% DI water at 1 mL/min for 6 min per sample. For benzotriazole samples, an eluent of 40% methanol/60% 5mM phosphate buffer at pH 7 was used at 1 mL/min for 7 min per sample, with analysis at 268 nm. Caffeine samples were analyzed at 273 nm with an eluent of 70% DI/30% methanol at 1 mL/min for 7 minutes. Carbamazepine samples were analyzed at 213 nm with an eluent of 45% acetonitrile/55% DI water at 1 mL/min for 6 min per sample. For DEET samples, an eluent of 40% acetonitrile/60% 5mM phosphate buffer, all adjusted to pH 3, was used at 1 mL/min for 9 min per sample, with analysis at 220 nm. Metoprolol samples were analyzed at 223 nm with an eluent of 22% acetonitrile/78% 5mM phosphate buffer at pH 5. Naproxen samples were analyzed at 231 nm with an eluent of 25% acetonitrile/75% 5 mM phosphate buffer adjusted to pH 7 at 1 mL/min for 6 minutes. For sulfamethoxazole samples, an eluent of 30% methanol/70% 5mM phosphate buffer at pH 5 was used at 1 mL/min for 9 min per sample, with analysis at 268 nm. Samples were analyzed using an Agilent ZORBAX Eclipse Plus C18 column. For all HPLC methods, injection volumes of 100 μL of each sample were used to ensure detection of low levels (ppb) of micropollutants.

SUPPLEMENTAL RESULTS AND DISCUSSION

Characterization results from composites prepared with 5 nm anatase TiO_2 nanoparticles. While the majority of studies were conducted with P25 particles, limited investigations were conducted with composites prepared using 5 nm anatase to explore the influence of TiO_2 particle size on composite properties and performance. In contrast with larger P25 particles, C/TiO_2 nanofiber composites prepared from 5 nm anatase TiO_2 nanoparticles were affected differently by the inclusion of PTA in sol gel. As shown in Figure S6, the surface morphology of C/50% 5 nm anatase TiO_2 with and without 2.5% PTA were comparable, with those nanofibers prepared with PTA showing virtually no introduced macroporosity in the nanofiber, though PTA did increase the nanofiber diameter (as seen with P25 composites) from 150 ± 50 nm to 230 ± 60 nm. Further, in comparing 50 wt.% TiO_2 composites prepared from 5 nm anatase or P25, TiO_2 exhibited a lower surface abundance in nanofibers prepared from 5 nm nanoparticles (~1 at.% surface Ti from XPS) relative to those prepared from P25 (~2 at.% surface Ti from XPS). This is likely the result of the greater aggregation state of the 5 nm particles, which limits their ability to more uniformly distribute themselves on the nanofiber surface. Sedimentation studies supported this, as 5 nm anatase TiO_2 nanoparticles aggregated and settled out of DMF more rapidly than P25 nanoparticles (Figure S7a).

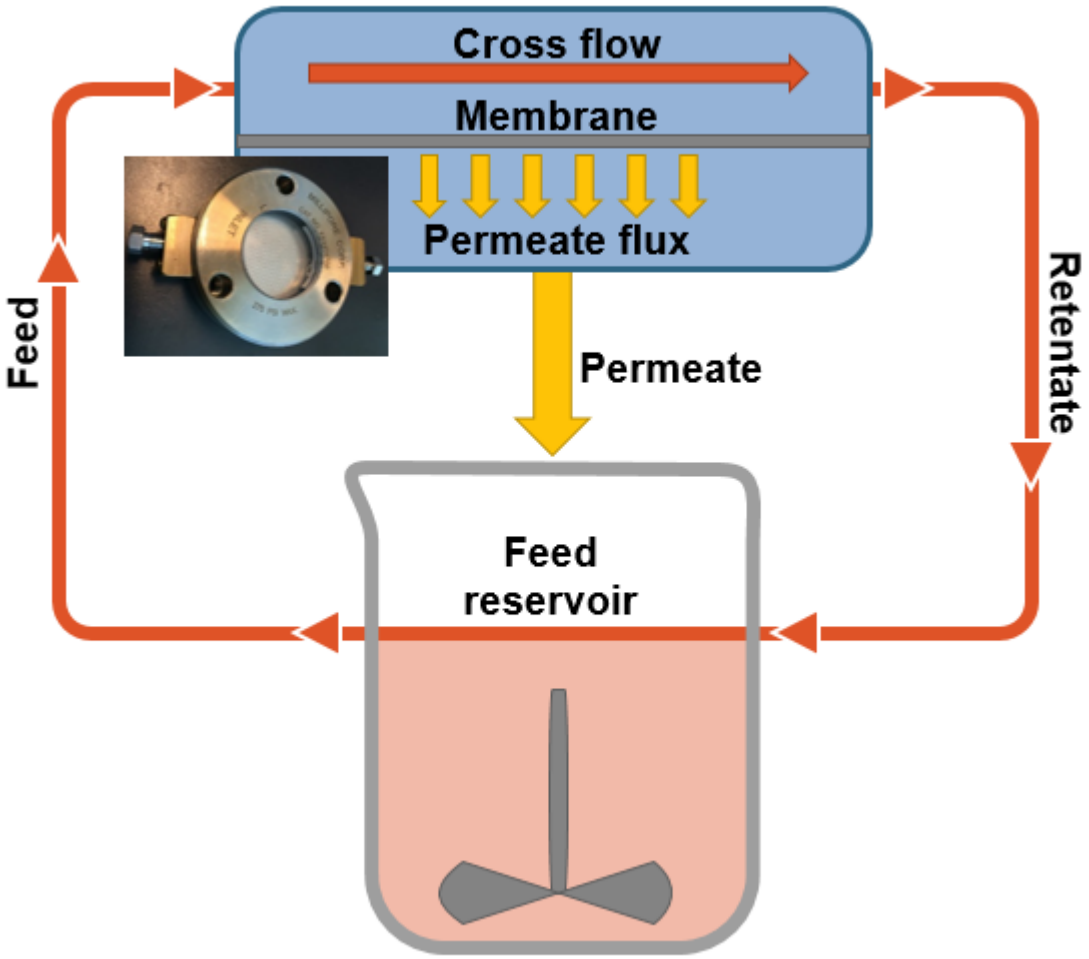

Figure S1. A schematic of the cross-flow filtration system used to test C/TiO_2 nanofibers in this study. The inset by the cross-flow membrane shows the Millipore filter holder modified with a quartz window and side inlet/outlet to allow for cross-flow filtration with exposure to UV light. Both retentate (cross-flow) and permeate (flow through the filter) were returned to the feed reservoir. Periodic samples were taken of permeate, retentate, and the reservoir during filtration experiments.

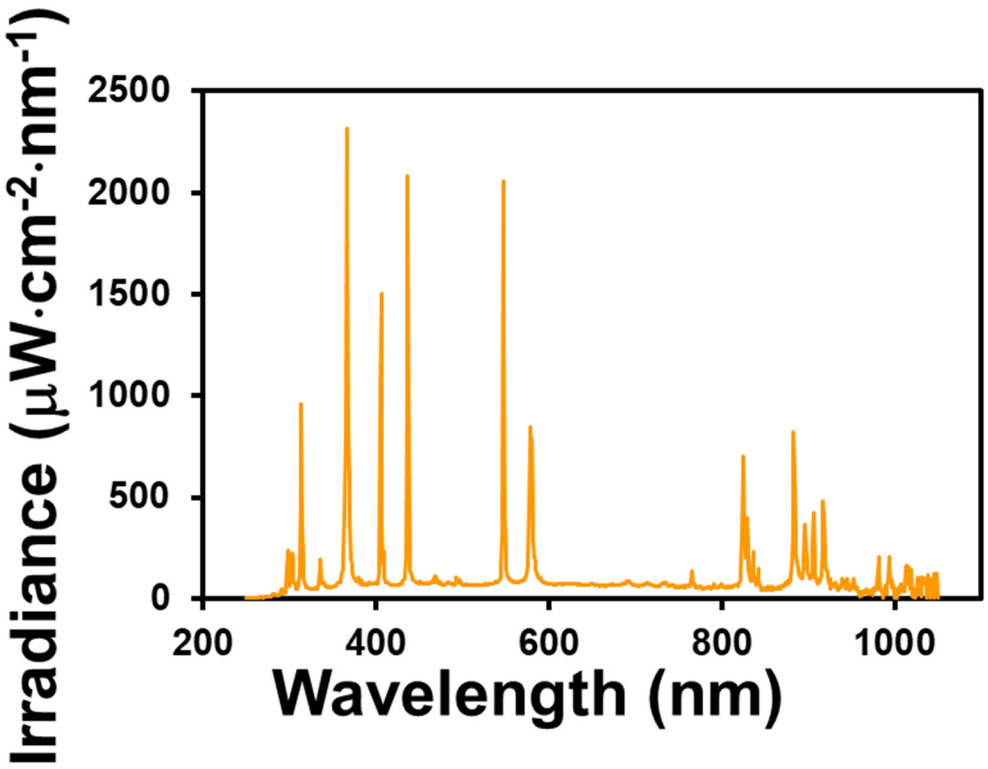

Figure S2. Irradiance spectra of the 250 W Newport XeHg lamp equipped with 250 nm cut-on filter. The output from this light source over 250-400 nm, most relevant to our experimental conditions, is 1.7×10-2 W cm^{-2}.

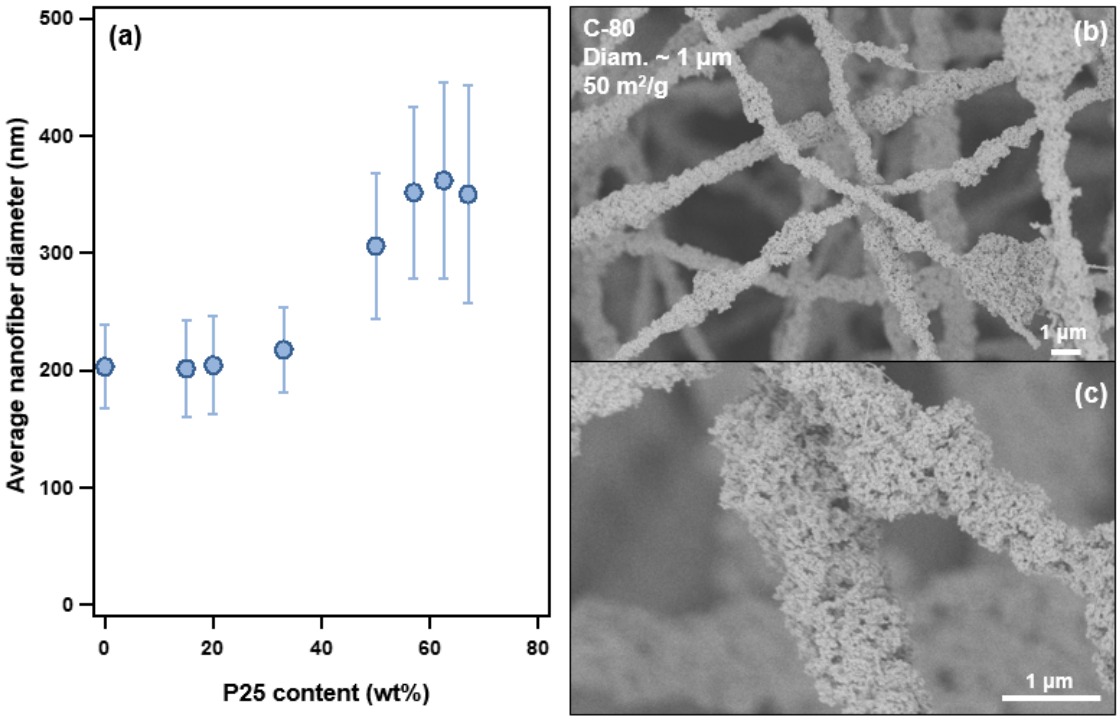

Figure S3. (a) Average nanofiber diameter is shown as a function of P25 content (wt. %) in C/TiO_2 nanofibers. (b and c) SEM images of C-80 which show nanofiber diameters of ~1 µm and extensive surface coverage with P25 nanoparticles.

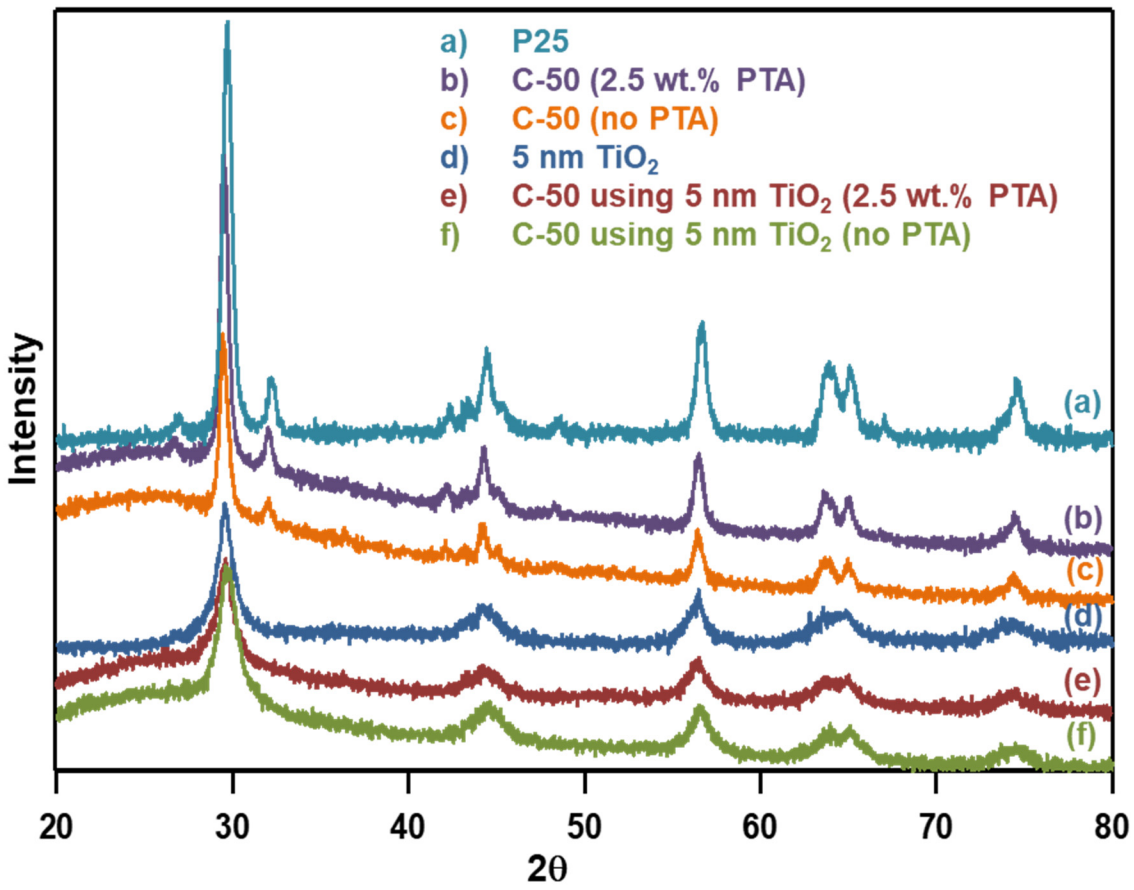

Figure S4. X-ray diffraction spectra for (a) P25 nanoparticles, (b) C-50 with 2.5 wt.% PTA, (c) C-50 (without PTA), (d) 5 nm anatase TiO_2 nanoparticles, (e) C-50 using 5 nm TiO_2 with 2.5 wt.% PTA, and (f) C-50 using 5 nm TiO_2 (without PTA). Electrospinning and stabilizing/carbonizing composites did not change the resultant XRD spectra of TiO_2 nanoparticles.

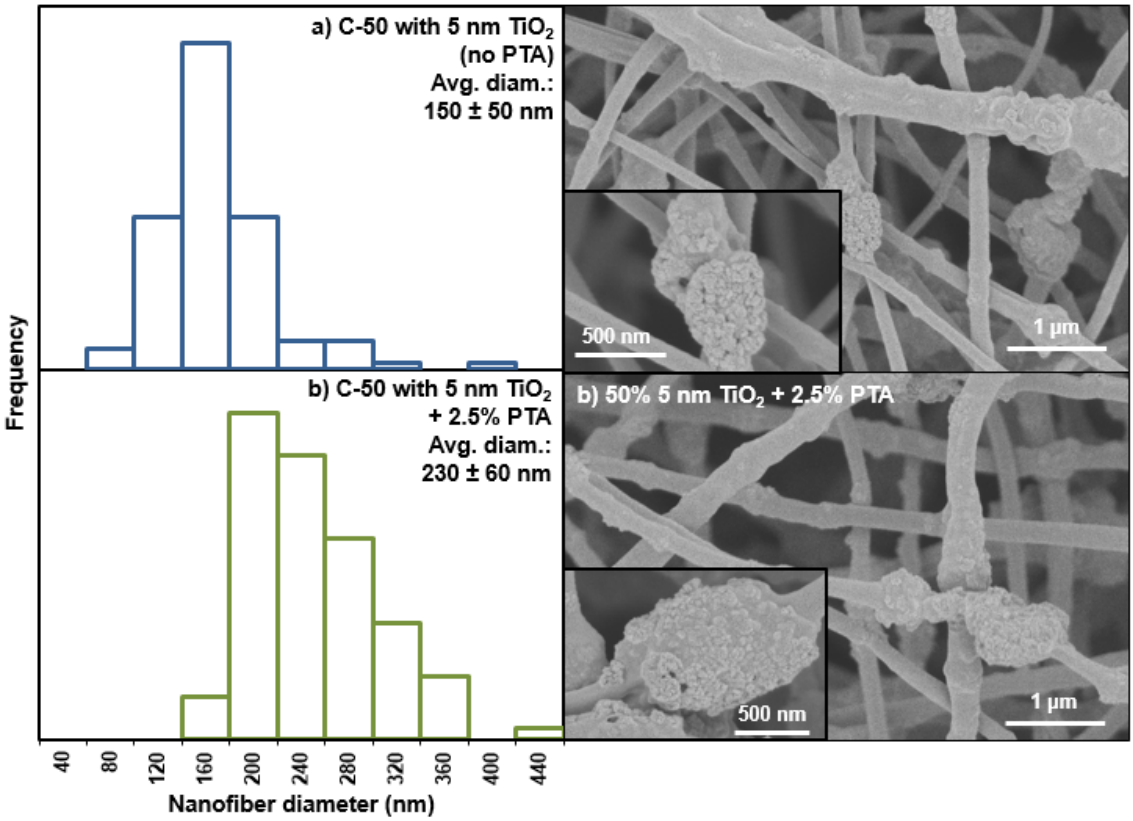

Figure S5. Histograms and associated SEM images of (a) C-50 using 5 nm anatase TiO_2 nanoparticles without PTA and (b) C-50 using 5 nm anatase TiO_2 nanoparticles with 2.5 wt.% PTA. SEM insets show aggregates of 5 nm TiO_2 in the composite nanofibers.

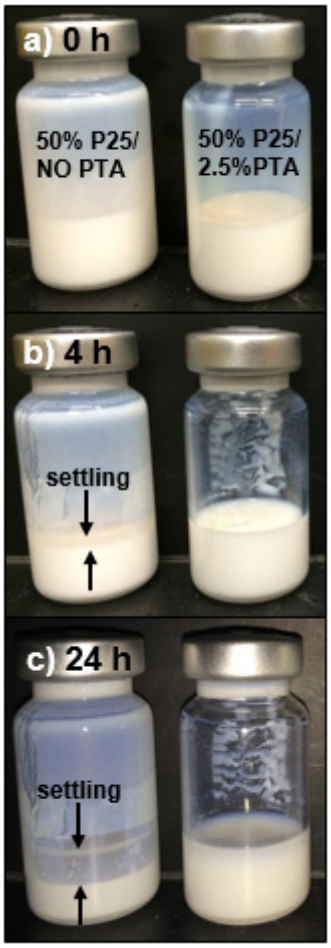

Figure S6. Electrospinning sol gels containing 50 wt.% P25 (relative to PAN that would be added) in DMF without PTA (left) and with 2.5 wt.% PTA (relative to final sol gel mass) after (a) initial preparation and 5 h of sonication (0 h), (b) 4 h, and (c) 24 h. P25 began to settle out, as indicated with arrows, after (b) 4 h and (c) 24 h without PTA present. Notably, 4 h after suspension preparation P25 began to settle out of solution when PTA was not present, and by 24 h the majority of P25 had settled out of the suspension. In contrast, P25 remained well-dispersed in DMF when PTA was present, resulting in a stable suspension throughout the 24 h observation period.

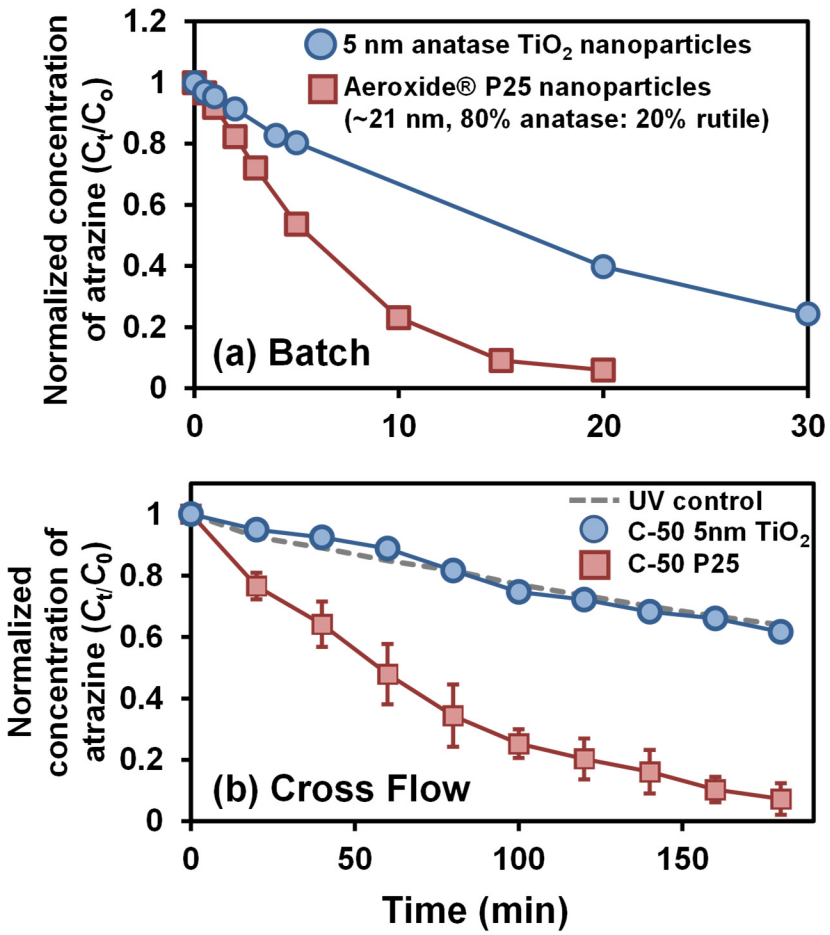

Figure S7. Normalized concentration of (a) 75 µM atrazine over time when reacted in batch suspensions containing 0.1 g/L P25 (shown in red) and 0.1 g/L 5 nm anatase TiO_2 (shown in blue) in 25 mL solution under UV light with wavelengths greater than and equal to 250 nm; and (b) 30 ppb atrazine over time for C/TiO_2 nanofiber composites with 50 wt.% P25 and with 5 nm TiO_2 nanoparticles used in place of P25. A UV control (conducted without TiO_2 material) is shown with the grey dashed line.

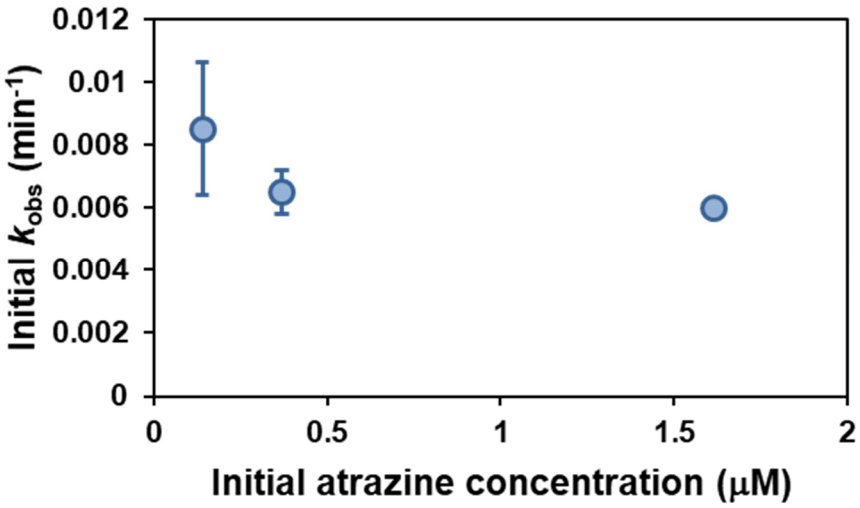

Figure S8. Initial k_{obs} with C-50 as a function of initial atrazine concentration, determined from the change in atrazine concentration in the reservoir over time. Notably, k_{obs} were roughly equivalent across the concentration range. Experiments were conducted at a flow rate of 10 mL/min across and through the filter.

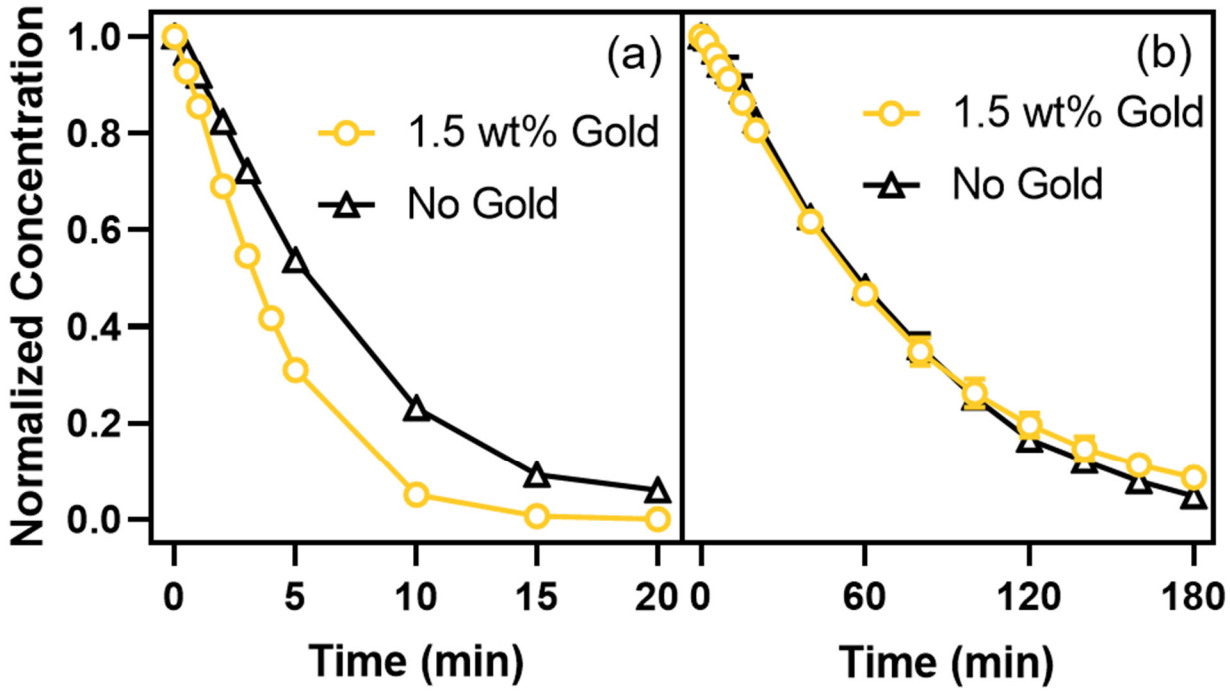

Figure S9. (a) Normalized concentration of atrazine (initial concentration of 100 μM) over time when reacted in batch suspensions of 0.1 g/L of Au/TiO_2 nanoparticles (shown in yellow) and 0.1 g/L of P25 nanoparticles (shown in black). Both suspensions were prepared in 25 mL solution under UV light with wavelengths greater than and equal to 250 nm. (b) Normalized concentrations of 0.5 μM atrazine over time when reacted in the flow-through UV filtration system using a C/TiO_2 nanofiber composite containing 50 wt.% Au/TiO_2 (shown in yellow) and a C/TiO_2 composite containing 50 wt.% P25 (shown in black).

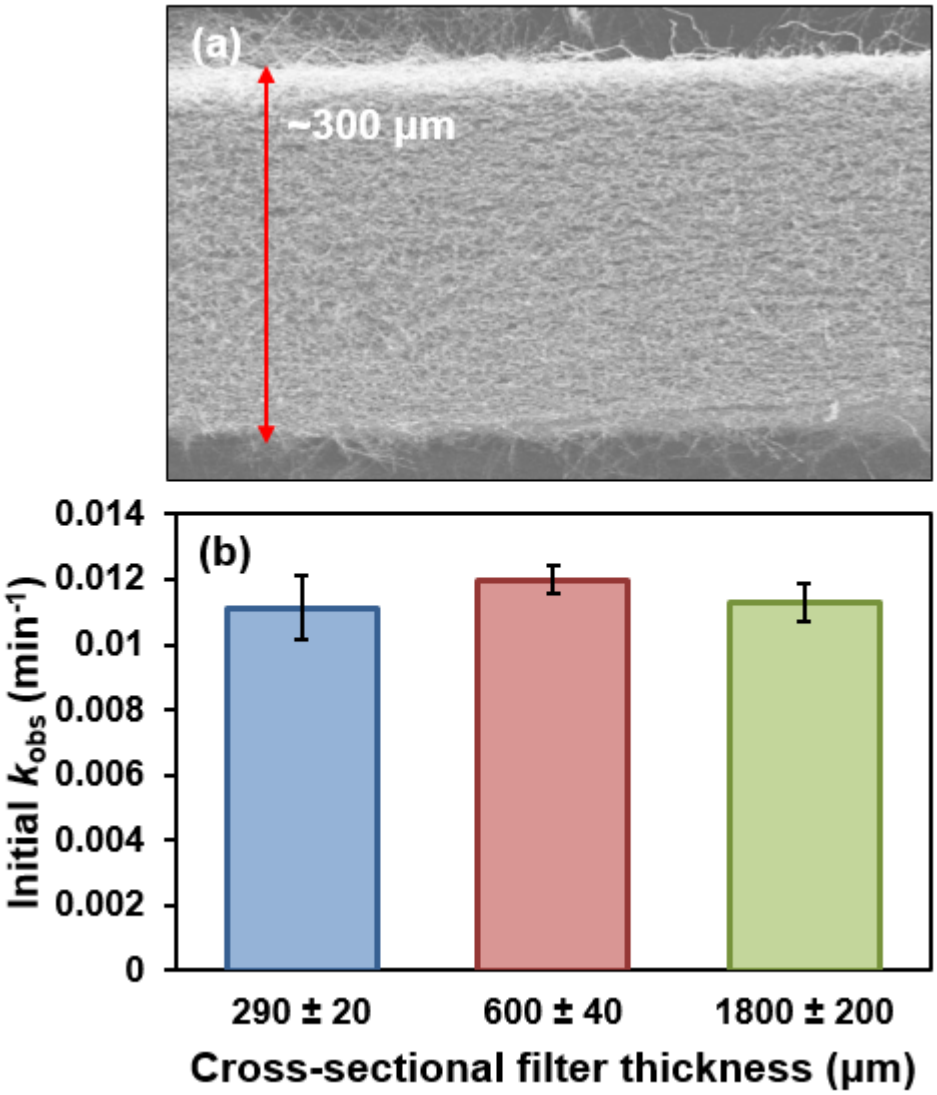

Figure S10. (a) SEM image of the cross-section of ~300 µm thick C-50 nanofiber filter. (b) Initial reaction rate coefficients for atrazine decay (k_{obs} values; determined from the change in atrazine concentration over time in the reservoir) as a function of cross-sectional filter thickness for C-50. Greater filter thicknesses corresponded with more mass. Experiments were conducted at a flow rate of 10 mL/min across and through the filter.

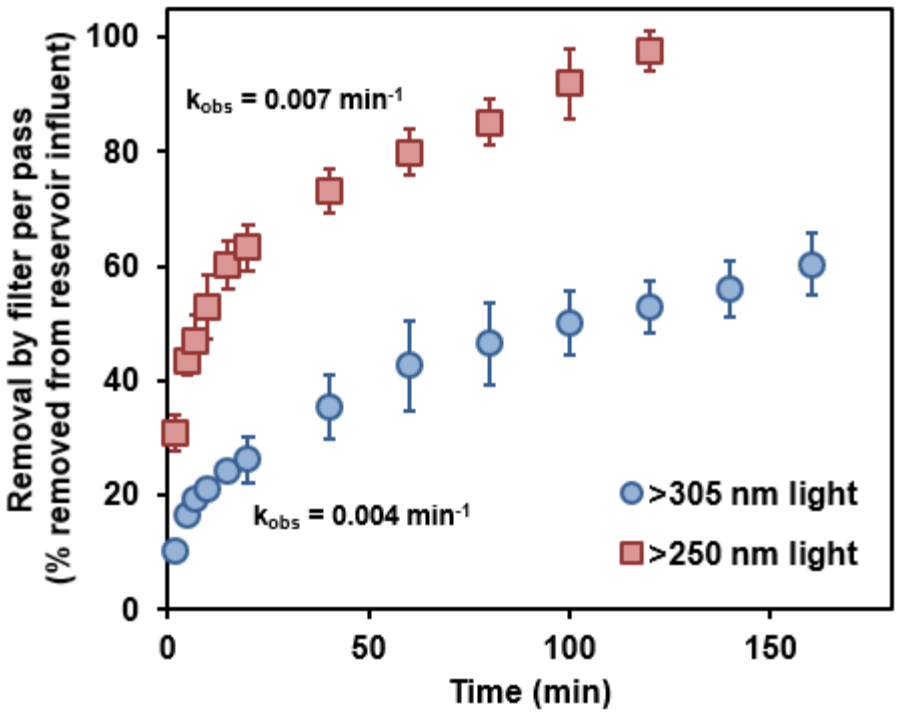

Figure S11. Removal of atrazine in a single filter pass (as measured by differences in atrazine concentration between filter influent and permeate) over time for experiments conducted with simulated sunlight [UV light greater than 305 nm in length (in blue)] and UV light greater than 250 nm in length (in red). Initial atrazine concentration was 0.5 μM. The use of UV light with smaller wavelengths resulted in more rapid removal, though removal between 20-50% per pass through the filter was still achieved using simulated sunlight (> 305 nm light). Experiments were conducted at a flow rate of 10 mL/min across and through the filter. Initial k_{obs} values are provided for comparison of each irradiation source, determined from the change of atrazine concentration over time in the reservoir.

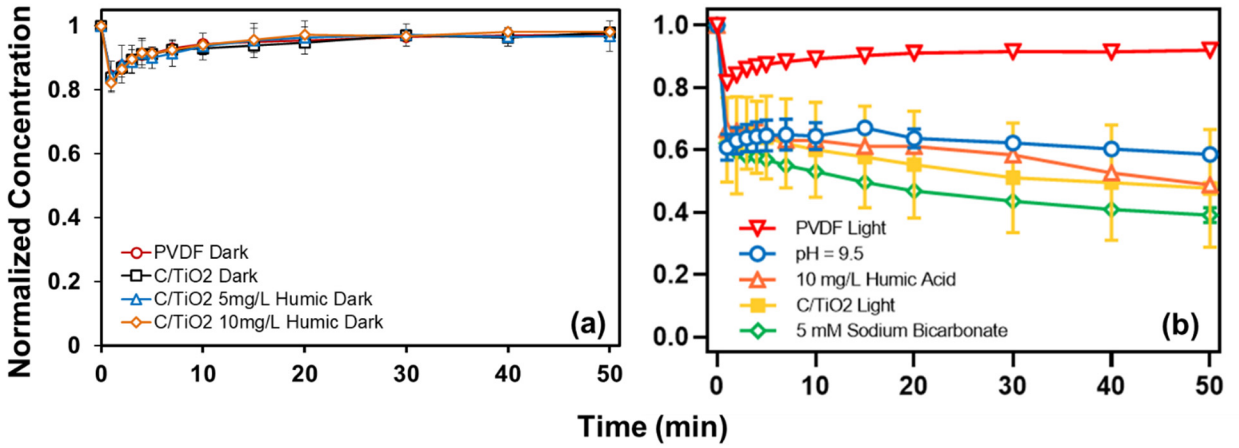

Figure S12. Normalized atrazine concentration (initial concentration of 0.5 μM) over time in the flow-through UV filtration system operated in a cross flow filtration mode without circulation (i.e., retentate and filtrate were not returned to the feed reservoir). Data are shown for 50 wt.% C/TiO_2 under (a) in the dark and (b) under UV light irradiation with wavelengths greater than and equal to 250 nm. In (a), we also include atrazine concentration over time data for a dark filtration system without C/TiO_2 to assess the influence of the filter PVDF support on atrazine removal. Dark control data are also shown for two systems in the presence of either 5 or 10 mg/L humic acid, which had no influence on atrazine losses in our control systems. Atrazine concentration data in (b) are also shown for irradiated filters when operated under a variety of solution phase conditions. In (b), data from a UV-only control (i.e., no C/TiO_2 and just the PVDF support) is shown in red. The typical experimental solution (5 mM phosphate buffer at pH 7) is shown in yellow, whereas other conditions more representative of authentic environmental systems include 5 mM phosphate buffer at pH 9.5 (shown in blue), 10 mg/L humic acid solution prepared at pH 7 in 5 mM phosphate buffer (shown in orange), and a 5 mM sodium bicarbonate solution at pH 7 (shown in green).

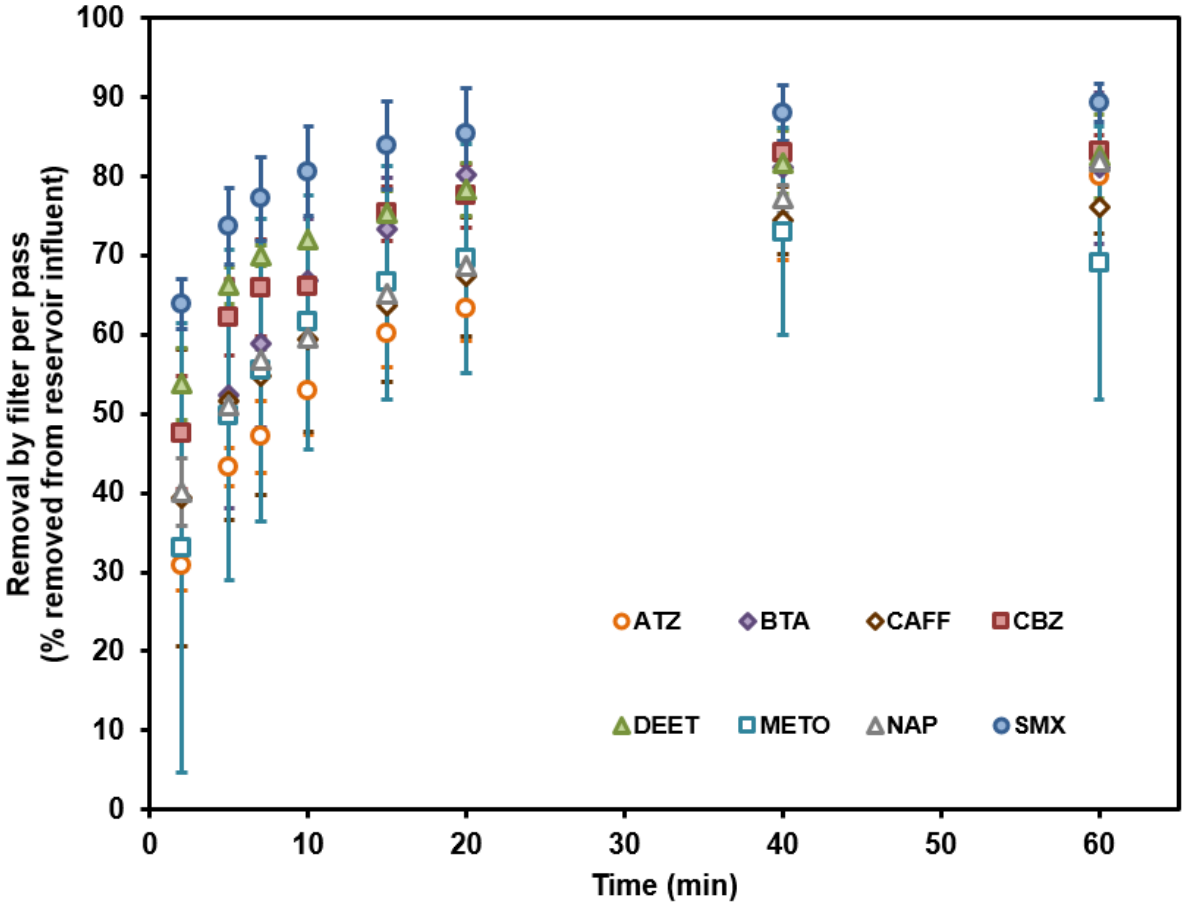

Figure S13. Removal by filter per pass (as measured by differences in contaminant concentration in filter influent and permeate) over time for atrazine (ATZ), benzotriazole (BTA), caffeine (CAFF), carbamazepine (CBZ), DEET, metoprolol (METO), naproxen (NAP), and sulfamethoxazole (SMX). Experiments were conducted in cross-flow, recirculating filtration mode at an initial concentration of 0.5 μM for all compounds and a flow rate of 10 mL/min both across and through the UV-irradiated filter layer.

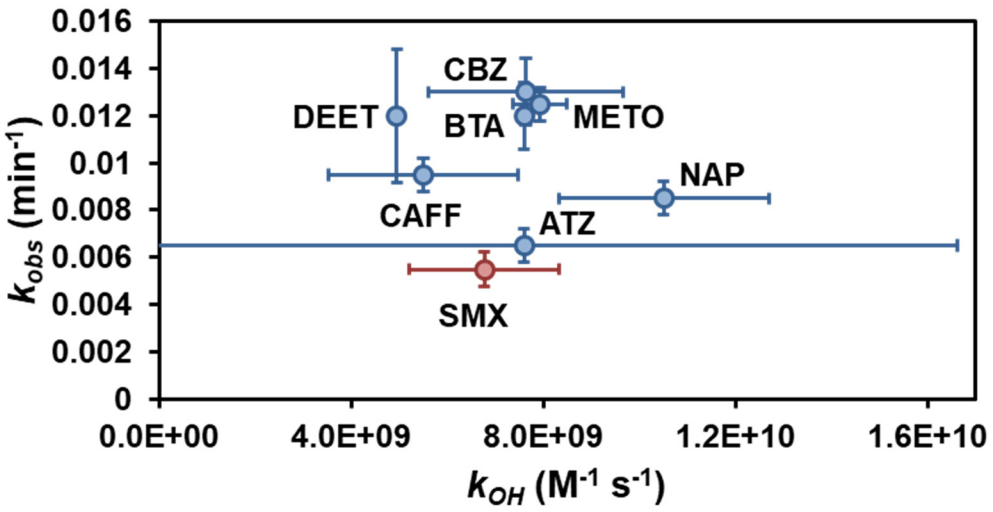

Figure S14. Initial reaction rate coefficients for atrazine (ATZ), benzotriazole (BTA), caffeine (CAFF), carbamazepine (CBZ), DEET, metoprolol (METO), naproxen (NAP), and sulfamethoxazole (SMX) as a function of their reported second order rate constants for hydroxyl radical. All hydroxyl radical rate constants (k_{OH}) are reported as mean values (with standard deviation) from values tabulated by Mandal.[3] Sulfamethoxazole is noted in red because its extensive direct UV photolysis in our system, which contributes to our measured k_s value.

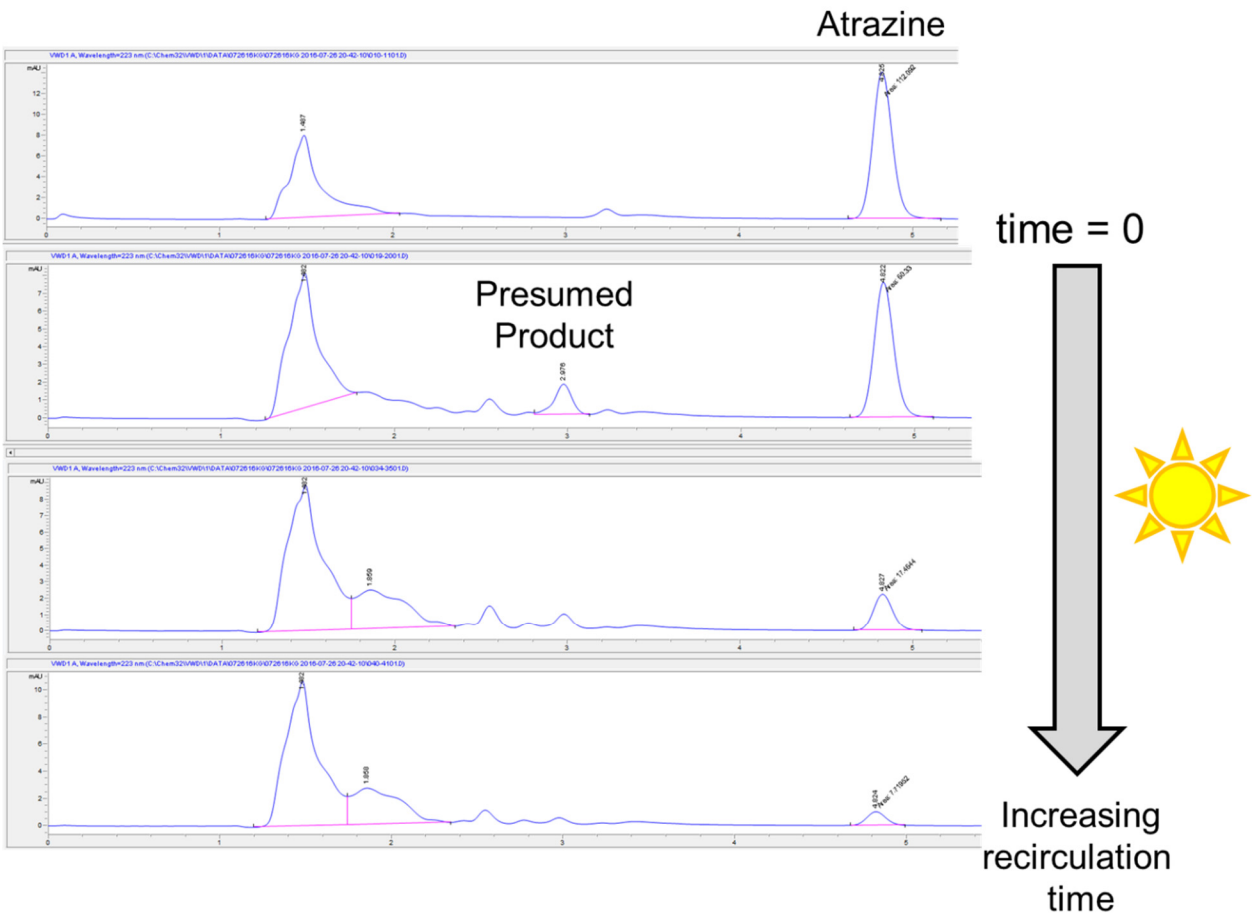

Figure S15. HPLC with diode array detection traces (λ = 223 nm) for a series of samples analyzed as a function of irradiation time during C/TiO_2 reaction with atrazine in a recirculating filtration system. With UV irradiation, the peak area for atrazine (at a retention time of ~4.8 min on our reverse phase C_{18} column) decreases over time. In all experiments with atrazine, a major, more polar product was initially observed (see peak at a retention time of ~3 min). Although this peak initially grew in peak area over early reaction timescales, it would eventually start to decrease (as shown here) over time. We presume it is further degraded to yield additional, more polar degradation productions (note the shoulder growing in over time at about 1.8 min adjacent to the peak eluting at 1.5 min, which corresponds to species unretained on the C_{18} column).

Literature Cited

(1) Nalbandian, M. J.; Greenstein, K. E.; Shuai, D.; Zhang, M.; Choa, Y. H.; Parkin, G. F.; Myung, N. V.; Cwiertny, D. M. Tailored Synthesis of Photoactive TiO2 Nanofibers and Au/TiO_2 Nanofiber Composites: Structure and Reactivity Optimization for Water Treatment Applications. *Environ. Sci. Technol.* **2015**, *49* (3), 1654–1663.

(2) Peter, K. T.; Vargo, J. D.; Rupasinghe, T. P.; De Jesus, A.; Tivanski, A. V; Sander, E. A.; Myung, N. V; Cwiertny, D. M. Synthesis, Optimization, and Performance Demonstration of Electrospun Carbon Nanofiber–Carbon Nanotube Composite Sorbents for Point-of-Use Water Treatment. *ACS Appl. Mater. Interfaces* **2016**, *8* (18), 11431–11440.

(3) Mandal, S. Reaction Rate Constants of Hydroxyl Radicals with Micropollutants and Their Significance in Advanced Oxidation Processes. *J. Adv. Oxid. Technol.* **2018**, *21* (1), doi: 10.26802/jaots.2017.0075